JOURNAL OF COMPUTATIONAL PHYSICS 100, 64–76 (1992)

Truncation Error Analysis of the Finite Volume Method for a Model Steady Convective Equation

YIH NEN JENG AND JIANN LIN CHEN

Department and Institute of Aeronautics and Astronautics, National Cheng Kung University, Tainan, Taiwan, Republic of China

Received January 31, 1990; revised June 17, 1991

A fundamental error relation inherent in the Gauss divergence theorem provided the basis for studying the truncation error of the finite volume method with cell center formulation for a model steady convective equation. The consistency of the classical first- and second-order upwind schemes are proved to be seriously dependent on the grid distribution. If the simple nature of the finite volume method is retained, it is found that a consistent scheme for convective terms can not avoid the dissipation due to grid nonuniformity. The geometrical interpretation of the diffusive terms such as $\nabla^2\phi$ are undertaken. Classical finite volume methods, which average an undefined ϕ from its neighbouring nodes, are shown to introduce false fluxes whenever grid nonuniformity is present. A simple modification is proposed to cancel the false fluxes. Two test cases for the Laplace equation illustrate the applicability of the proposed scheme. However, even with this modified scheme, the consistency problem of the diffusion term is found to be seriously dependent on the grid uniformity.

1. INTRODUCTION

The finite volume method for partial differential equations is widely used in scientific and engineering applications, since they are relevant to physical problems and can avoid geometrical singularities. Specifically, much attention was directed to the following convective equations: Burgers equation, Euler equations, and the Navier–Stokes equations [1].

Before one can prove the convergence of numerical methods for a certain differential equation, the consistency conditions should have been previously met by virtue of Lax's equivalence principle [2]. Consequently, truncation error analysis is extensively studied. Before 1968 [3–5], research related to nonuniform grid systems centered on one-dimensional analyses. Several subsequent papers [6–8] focused on the properties of the truncation error on nonuniform grids. Although all of them were one-dimensional analyses, they theoretically built in theory for the multiple-dimensional framework in which we now work.

In the mid 1980s, different opinions between Hirt and Ramshaw [9] and Roache [10] raised the following question: should the truncation error analysis be performed on the physical domain or on the computational domain [11]? So far, the existing approaches do not give a definite answer. As in previous works [3–8], Hoffman [11] prefers neither the physical nor the computational domain. Thompson and his colleagues [12, 13] and Lee and Tuesi [14] performed their analyses on the computational domain. However, Veuillot and Viviand [15], Pike [16], Turkel [17, 18], Turkel and his colleagues [19], Roe [20], Giles [21], Wang and Widhopf [22], Radespiel and Swanson [23], and Morton and Paisley [24] all used physical domain analyses.

In fact, the key to Hirt, Ramshaw, and Roache's question already existed in earlier works [6–8, 11]. For a one-dimensional approach, consider the following derivatives with central difference approximation [6–8, 11],

$$(\phi_x)_j = \frac{\phi_{j+1}-\phi_{j-1}}{x_{j+1}-x_{j-1}} - \frac{1}{2}(\phi_{xx})_j \times [x_{j+1}-2x_j+x_{j-1}] + O(\Delta x_j^2)$$

$$[(\tau\phi_x)_x]_j = \frac{2}{x_{j+1}-x_{j-1}}\left[\tau_{j+1/2}\frac{\phi_{j+1}-\phi_j}{x_{j+1}-x_j} - \tau_{j-1/2}\frac{\phi_j-\phi_{j-1}}{x_j-x_{j-1}}\right] - \frac{1}{12}[\tau\phi_{xxx}+3(\tau\phi_x)_{xx}]_j \times [x_{j+1}-2x_j+x_{j-1}] + O(\Delta x_j^2), \quad (1)$$

where ϕ and τ are variables, $\phi_x = \partial\phi/\partial x$, ..., and $(\ )_j$ denotes variable at jth spatial nodal point, and $\Delta x_j = 0.5(x_{j+1}-x_{j-1})$, etc. Similar relations can be written without difficulty for a one-sided differencing scheme. By discrete mapping from $\{x_j\}$ to $\{\xi_j\}$, Eq. (1) is rewritten as

$$(\phi_x)_j = \left[\left(\frac{\phi_\xi}{x_\xi}\right)_j + O(\Delta\xi_j^2)\right] - \frac{1}{2}(\phi_{xx})_j[x_{j+1}-2x_j+x_{j-1}] + O(\Delta x_j^2)$$

0021-9991/92 $5.00

$$[(\tau\phi_x)_x]_j = \left[\left[\frac{(\tau\phi_\xi/x_\xi)_\xi}{x_\xi}\right]_j + O(\Delta\xi_j^2)\right] - \frac{1}{12}[\tau\phi_{xxx} + 3(\tau\phi_x)_{xx}]_j \times [x_{j+1} - 2x_j + x_{j-1}] + O(\Delta x_j^2) \tag{2}$$

in which $(\ )_\xi = \partial(\ )/\partial\xi$. Clearly, if

$$[x_{j+1} - 2x_j + x_{j-1}] \sim O(\Delta x_j^2) \tag{3}$$

then the following reciprocal relations exist:

$$\begin{aligned}(\phi_x)_j + O(\Delta x_j^2) &= \left(\frac{\phi_\xi}{x_\xi}\right)_j + O(\Delta\xi_j^2) \\ [(\tau\phi_x)_x]_j + O(\Delta x_j^2) &= \left[\frac{(\tau\phi_\xi/x_\xi)_\xi}{x_\xi}\right]_j + O(\Delta\xi_j^2).\end{aligned} \tag{4}$$

In other words, the error analysis on both the computational and the physical domain will be equivalent, if Eq. (3) is valid. Therefore, before a reciprocal relation like Eq. (4) has been proved, a second-order scheme on the physical domain cannot necessarily be taken to be second order on the computational domain and vice versa. This conclusion applies to both the finite difference and the finite volume methods.

In spite of its increasing importance, additional work done on the behavior of the finite volume method on nonuniform mesh did not surface until 1985. Turkel and his coworkers [17–19] did the first systematic study of truncation error for the finite volume method on nonuniform meshes. The analysis was done on the physical rather than the computational domain, due to the former's relatively straightforward condition of derivation. Turkel, using the cell center formulation, found that many schemes reduce to first-order accuracy and would be inconsistent on nonsmooth grid systems. Roe [20] performed the analysis for cell vertex formulation and constructed a scheme that is insensitive to grid stretching. Morton and Paisley [24] extended Turkel's idea to solve the Euler equations. They compared cell center and cell vertex formulations and found that the latter is again less sensitive with respect to grid distortion. Radespiel and Swanson [23] also employed two formulations for the Navier–Stokes equations and found that these did not significantly differ. Wang and Widhopf [22] successfully extended Turkel's idea on the physical domain to construct their TVD scheme.

Note that truncation error analysis is only a local phenomenon.[1] A large local truncation error does not necessarily induce a significantly large solution error, as has been proven numerically by Flores *et al.* [25] and Lindquist and Giles [26]. By assuming that the solution error is of the same order as the truncation error and using spectral analysis, Giles [21] showed that high order accuracy can be achieved by careful numerical smoothing. Recently, Süli [27–29] performed a series of studies about the global stability, accuracy, and convergence of the finite volume method for both linear hyperbolic equations and the Poisson equation on distorted meshes. He found the distortion significantly affects both stability and accuracy. Moreover, he derived an estimation of the solution error which is principally determined by the truncation error.

Since the study of the truncation error of the finite volume method is relatively new, the phenomena has not been studied thoroughly. To the author's knowledge, error of the line integral part of the Gauss divergence theorem has not yet been fully examined. This paper will study the effect of this discretization on the error of a finite volume method with cell center formulation for a convective equation. The extension to that of cell vertex formulation is straightforward. For convenience, the governing equation will focus on a two-dimensional model convective equation. Note that the present truncation error analysis is only suitable for smooth solutions and that it may become meaningless in regions of discontinuity. Besides the above reciprocal relations of Eq. (4), the question of the existence of other important criteria for the finite volume method will be examined. The present analysis will focus on the physical domain, since condition (3) and the governing equation originated thereon.

Although all the symbols are properly explained in the text, for the sake of clarity three types of subscripts are herewith explicated:

1. $(\ )_x$, where "x" can be single or multiple letters of "x, y" or "ξ," denoting a derivative with respect to the subscript.

2. $(\ )_a$, where "a" can be a single or double letter (or number) other than x, y, ξ. This is a variable at the nodal point denoted by the subscript.

3. $\Delta(\ )_{ab}$, where "a" and "b" are none of "x, y, ξ." This symbol denotes a difference measured from point "a" to point "b". If either "a" or "b" is composed of double letters, a dashed line is added to make the expression clear. For example, $\Delta x_{P\_WW} = x_{WW} - x_P$.

In Section 2, the fundamental lemma of discretizing the line integral part of the Gauss divergence theorem will be considered first. Errors of the first- and second-order upwind schemes will also be discussed on uniform and nonuniform grid systems using this lemma. A systematic analysis of the diffusive term will be performed, and a method to deal with it will be proposed. In Section 3, five schemes, including the proposed one, will be applied to test two problems governed by the Laplace equation.

[1] The authors are grateful to one of the referees who pointed out this fact.

2. ANALYSIS

The fundamental theorem for the finite volume method is the Gauss divergence theorem [30], which is defined on continuous space. Before we go into more detail, the error behavior induced by the discretization of the theorem's line integral will be studied first. This is described in a lemma on which all the subsequent theoretical developments of the present analysis will be based.

2.1. A Fundamental Lemma of Truncation Error

Consider a polygonal control volume $1234\cdots1$ as shown in Fig. 1a, where the circle denotes the centroid of the control volume, and the star denotes the center of each side of the control surface. The Gauss divergence theorem [30] is

$$\int_A \nabla\cdot\mathbf{V}\,dA=\oint \mathbf{V}\cdot d\mathbf{s} \tag{5}$$

in which A is the area of the control volume and s is the arc length along the control surface, so that

$$\mathbf{V}=u\mathbf{i}+v\mathbf{j}, \tag{6}$$

where $\mathbf{i}$, $\mathbf{j}$ are unit vectors in directions x, y, respectively, and u, v may be either corresponding velocity components or derivatives of functions.

The finite volume method evaluates the RHS of Eq. (5) numerically to approximate the average of $\nabla\cdot\mathbf{V}$ within the area "A". Note that u, v of the LHS of Eq. (5) are cell-averaged quantities and are not known at specific points. Therefore, the problem in defining the truncation error explicitly was an open question for many years. To overcome this difficulty, Turkel [17] represented the integral by a point value $(\nabla\cdot\mathbf{V})_P$ to obtain

$$\begin{aligned}\int_A \nabla\cdot\mathbf{V}\,dA &= [(u_x)_P+(v_y)_P]A+O(A^2)\\ O(A^2) &= [(u_{xxx})_P+(v_{xxy})_P]\int_A \frac{(x-x_P)^2}{2}\,dA+\cdots,\end{aligned} \tag{7}$$

where the subscript "P" denotes the location at the centroid of "A". The second-order terms u_{xx}, ... disappear because of the definition of centroid x_P, y_P of a cell. Note that this term, $O(A^2)$ obtained from Turkel's approximation, corresponds to the error of Newton–Cotes' integration formula [31].

With the help of Eq. (7), the RHS discretizing error of Eq. (5) can be found. Once the approximation of the line integral of Eq. (5) is determined, the difference between its Taylor series expansion (with respect to central point "P") and Eq. (7) can be found. This value is called the truncation error. For the sake of simplicity, only the errors up to second order will be considered in this study.

Assume that a finite volume method approximates the RHS of Eq. (5) by

$$\begin{aligned}\text{Discrete}\left[\oint \mathbf{V}\cdot d\mathbf{s}\right] &= u_a\,\Delta y_{12}-v_a\,\Delta x_{12}+u_b\,\Delta y_{23}\\ &\quad -v_b\,\Delta x_{23}+u_c\,\Delta y_{34}-v_c\,\Delta x_{34}\\ &\quad +\cdots,\end{aligned} \tag{8}$$

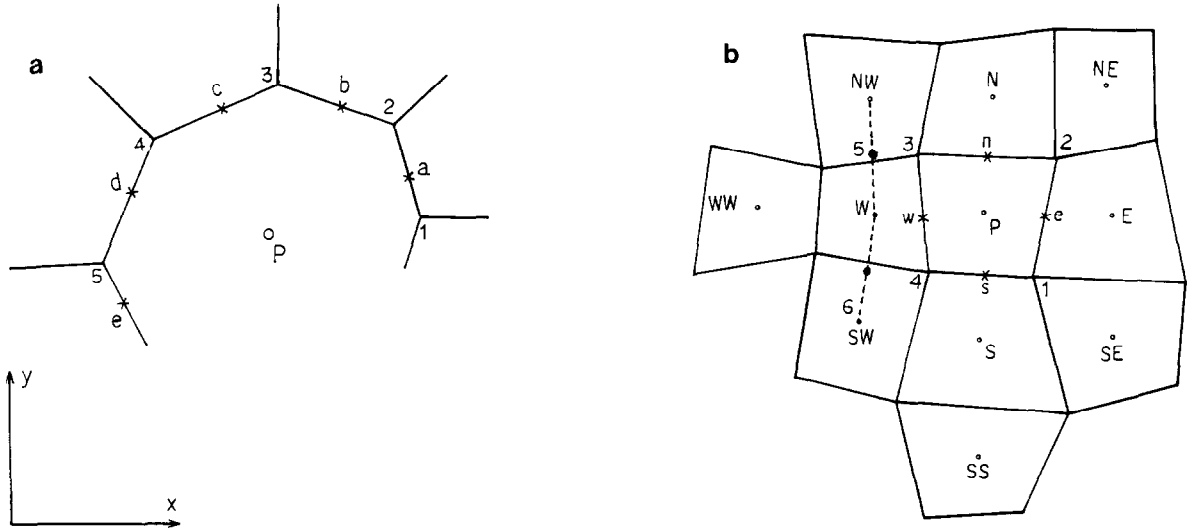

FIG. 1. (a) The control volume on the physical domain. (b) The grid arrangement on the physical domain.

where subscript "a" indicates the center of boundary $\overline{12}$, "b" the center of $\overline{23}$, etc., as shown in Fig. 1a, while $\Delta y_{12} = y_2 - y_1$ and $\Delta x_{12} = x_2 - x_1$, etc. Note that the point values u_a, v_a, ... are considered as approximations to the mean values on corresponding cell boundaries. The error of Eq. (8), which does not include the error of evaluating $u_a \cdot v_a$, ..., can be expressed as

$$\begin{aligned}\text{Error} = &\frac{\Delta y_{12}}{12}\left[\frac{(u_{xx})_a}{2}\Delta x_{12}^2 + (u_{xy})_a \Delta x_{12}\Delta y_{12} + \frac{(u_{yy})_a}{2}\Delta y_{12}^2\right] \\ &- \frac{\Delta x_{12}}{12}\left[\frac{(v_{xx})_a}{2}\Delta x_{12}^2 + (v_{xy})_a \Delta x_{12}\Delta y_{12} + \frac{(v_{yy})_a}{2}\Delta y_{12}^2\right] \\ &+ \cdots = O(A^{1.5}). \end{aligned} \tag{8a}$$

Again, this error is the error of the Newton–Cotes open-end integration formula [31]. The terms u_x, ... disappear because of the definition of the central point of a line segment.

Now suppose that *"u" and "v" at the centroid of every control volume are known*, so that u_a, v_a, ... should be approximated by nodal values such as $u_a = \frac{3}{2}u_P - \frac{1}{2}u_W$ (with the symbols shown in Fig. 1b). After performing the Taylor series expansion with respect to points a, b, c, ..., respectively, these approximations of u_a, v_a, ... can be written as

$$\begin{aligned}\overline{u_a} &= u_a + \alpha_{0a}u_a + \alpha_{1a}(u_x)_a + \alpha_{2a}(u_y)_a \\ &\quad + \alpha_{3a}(u_{xx})_a + \alpha_{4a}(u_{xy})_a + \alpha_{5a}(u_{yy})_a + \cdots \\ \overline{v_a} &= v_a + \beta_{0a}v_a + \beta_{1a}(v_x)_a + \beta_{2a}(v_y)_a \\ &\quad + \beta_{3a}(v_{xx})_a + \beta_{4a}(v_{xy})_a + \beta_{5a}(v_{yy})_a + \cdots \\ &\quad \cdots, \end{aligned} \tag{9}$$

where the terms multiplied by α_{ia}'s and β_{ia}'s are the errors. The coefficients α_{ia}, ... are somewhat like Δx_{12}, ... in the Taylor series expansion. α_{0a} and β_{0a} are either zero or of the same order as α_{1a}, β_{1b}, respectively.

In general, the finite volume method defined by Eq. (8) may include two errors: (1) the error of Eq. (8a), due to approximation of the line integral on cell boundaries, and (2), that of evaluating u_a, v_a, ..., as shown in Eq. (9). For convenience, these errors are summarized in the following fundamental lemma.

LEMMA. *Let the approximations to u_a, v_a, ... be expanded as in Eq. (9). Suppose the RHS of Eq. (5) is approximated by Eq. (8). Then the truncation error is*

$$\begin{aligned}\text{Error} = &u_P(\alpha_{0a}\Delta y_{12} + \alpha_{0b}\Delta y_{23} + \alpha_{0c}\Delta y_{34} + \cdots) \\ &+ (u_x)_P[(\alpha_{0a}\Delta x_{Pa} + \alpha_{1a})\Delta y_{12} \\ &+ (\alpha_{0b}\Delta x_{Pb} + \alpha_{1b})\Delta y_{23} + \cdots] \\ &+ (u_y)_P[(\alpha_{0a}\Delta y_{Pa} + \alpha_{2a})\Delta y_{12} \\ &+ (\alpha_{0b}\Delta y_{Pb} + \alpha_{2b})\Delta y_{23} + \cdots] \\ &+ (u_{xx})_P\left[\left(\frac{\Delta x_{Pa}^2}{2}(1+\alpha_{0a}) \right.\right. \\ &\left.\left. + \alpha_{1a}\Delta x_{Pa} + \alpha_{3a}\right)\Delta y_{12} + \cdots\right] \\ &+ \cdots \\ &- v_P(\beta_{0a}\Delta x_{12} + \beta_{0b}\Delta x_{23} + \beta_{0c}\Delta x_{34} + \cdots) \\ &+ \cdots \end{aligned} \tag{10}$$

where the coefficients of the second and higher order derivatives include the terms of the integration error in Eq. (8a). Similarly, the error can also be expressed in terms of the order of Δx, Δy,

$$\begin{aligned}\text{Error} = &[\alpha_{0a}u_P + \alpha_{1a}(u_x)_P + \alpha_{2a}(u_y)_P \\ &+ \alpha_{3a}(u_{xx})_P + \alpha_{4a}(u_{xy})_P + \cdots]\Delta y_{12} \\ &- [\beta_{0a}v_P + \beta_{1a}(v_x)_P + \beta_{2a}(v_y)_P \\ &+ \beta_{3a}(v_{xx})_P + \beta_{4a}(v_{xy})_P + \cdots]\Delta x_{12} \\ &+ \cdots \\ &+ [\alpha_{0a}(u_x)_P + \alpha_{1a}(u_{xx})_P \\ &+ \alpha_{2a}(u_{xy})_P + \cdots]\Delta x_{Pa}\Delta y_{12} \\ &+ \cdots \end{aligned} \tag{11}$$

Proof. After substituting the expansions of Eq. (9) into Eq. (8), the result is expanded with respect to point "P." Subsequently, by subtracting the resulting equation from Eq. (7), Eqs. (10) and (11) are obtained. Q.E.D.

From the point of view of the order of the derivative, Eq. (10) indicates that the finite volume method amplifies the error. On the other hand, from the consistency point of view, the order of the error is equal to the order of the first nonzero error term in Eq. (11).

The lemma indicates that the consistency between the discretized line integral of Eq. (8) and the LHS of Eq. (5), significantly depends on the grid distribution and the approximating forms of u_a, v_a, ... Note that the midpoint integration rule for the convective term of the one-dimensional model equation, derived by Turkel and his coworkers [17–19], is in some sense similar to the present lemma.

If the known values of u, v are located at points 1, 2, ...

(see Fig. 1b), the error will be reduced to the Newton–Cotes closed-end integration error [31], similar to Eq. (8a). This conclusion is consistent with the results of Roe [20] and Morton and Paisley [24], in that cell vertex formulation is better than the cell center formulation for the Euler equations. However, the results of calculating the unsteady conservation equations are often represented at centroids, so that proper interpolation should be made so as to find $u_1, u_2, \ldots$ of Fig. 1b from u, v at these central points [32, 33]. If the computational stability problem can be solved, such as in Reddy and Jacocks' central difference scheme [34] and in Jameson and Mavriplis' scheme [33] with artificial viscosity, this type of a finite volume method would be excellent for the Euler equations; otherwise one has to properly interpret the upwind scheme for the convective terms. Note that this type of finite volume method still has intrinsic artificial viscosity due to the integration error of Eq. (8a).

As for the diffusive terms of the Navier–Stokes equations, u, v become derivatives, and the errors of Eq. (9) still exist. We will postpone discussion of this until Section 2.5.

Another possible approach, reminescent of the staggered grid scheme [35], places the known values of u, v at central points of line segments of control surfaces $a, b, c, \ldots$ of Fig. 1a or $e, n, w, s, \ldots$ of Fig. 1b. In both cases, the errors are similar to those mentioned in the previous paragraph and the interpretation of the upwind scheme is relatively easy. The method for finding $u_e, u_n, \ldots$ from $u_P, \ldots$, and the problems associated with the diffusive terms were solved in an analogous manner to the previous scheme.

Without loss of generality, the rest of this study will focus on the quadrilateral control volume (see Fig. 1b). Most of the results can be easily extended to a general polygonal control volume. For the sake of completeness, the uniform grid system is discussed first.

2.2. Truncation Error on Uniform Quadrilateral Grid Systems

In uniform quadrilateral mesh cases which are not restricted to rectangular grids, the symmetric character ($\Delta x_{12} = -\Delta x_{34}, \Delta y_{12} = -\Delta y_{34} \cdots$) plays an important role. It makes the order of accuracy of the closed loop integration of Eq. (10) equal to the order of accuracy of evaluating u_a, $v_a, \ldots$ of Eq. (9). It is interesting to note that while uniform meshes can only be constructed from either triangles, tetragonals, or hexagonals, those constructed from triangles [20] lack symmetric character.

For simplicity, we will use the first-order upwind scheme to represent $\mathbf{V}$ for a uniform rectangular grid system and assume that $u > 0$, $v > 0$, so that $\overline{u_e} = u_P$, $\overline{v_n} = v_P$, $\overline{u_w} = u_W$, $\overline{v_S} = v_S$, where the subscripts e, n, w, s denote the centers of corresponding control surfaces, and the subscripts P, W, S denote the centroids of corresponding control volumes as shown in Fig. 1b. From the Taylor series expansions of $\overline{u_e}, \ldots$ and by applying the fundamental lemma, the error of the closed loop integration of Eq. (5) becomes

$$\text{Error} = \Delta x\, \Delta y\, [-\tfrac{1}{2}(\Delta x\, (u_{xx})_P + \Delta y\, (v_{yy})_P) + \cdots]. \tag{12}$$

Note that the error terms corresponding to all the first-order derivatives $u_x, u_y, \ldots$ vanish and the error of the Newton–Cotes integration of Eq. (8) is improved to be $(\Delta x^3\, \Delta y/6)(u_{xxx})_P + (\Delta x\, \Delta y^3/6)(v_{yyy})_P \cdots$, all due to the symmetric character of the rectangular grid system.

On the other hand, if a nonuniform grid system is introduced, the symmetric character disappears and the coefficients α_i, β_i would be of order Δx, or Δy. As a consequence, the consistency problem on the physical domain may become large enough to pose a serious problem. This situation will be discussed in more detail in the next section.

2.3. The Model Convective–Diffusive Equation

Consider the model convective–diffusive equation which can represent most of the characters in the Navier–Stokes equations. This equation is written in integral form for a general quadrilateral cell (see Fig. 1b) and given below as

$$\oint_S \phi \mathbf{V} \cdot d\mathbf{S} = \oint_S \nabla\phi \cdot d\mathbf{S}, \tag{13}$$

where the LHS is the convective term; the RHS is the diffusive term; $\mathbf{V}$ is velocity vector; ϕ may be u, v, temperature, concentration, or any other variable; S is the enclosed boundary of the control volume; and $\mathbf{S}$ includes its outward normal.

2.4. The Determination of the Error of the Finite Volume Method for Convective Terms of the Model Equation

The convective transport is modelled by the classical first-order upwind scheme, by assuming positive contravariant velocities at points e, n, w, and s. After obtaining an expression comparable to Eq. (9), the error of the convective term will have become

$$\begin{aligned}\text{Error} = {} & [(\phi u)_x]_P\, [\Delta x_{PW}\, \Delta y_{34} + \Delta x_{PS}\, \Delta y_{41} - A] \\ & + [(\phi u)_y]_P\, [\Delta y_{PW}\, \Delta y_{34} + \Delta y_{PS}\, \Delta y_{41}] \\ & - [(\phi v)_x]_P\, [\Delta x_{PW}\, \Delta x_{34} + \Delta x_{PS}\, \Delta x_{41}] \\ & - [(\phi v)_y]_P\, [\Delta y_{PW}\, \Delta x_{34} + \Delta y_{PS}\, \Delta x_{41} + A] \\ & + \tfrac{1}{2}[(\phi u)_{xx}]_P\, [\Delta x_{PW}^2\, \Delta y_{34} + \Delta x_{PS}^2\, \Delta y_{41} + \cdots] \\ & + \cdots, \end{aligned} \tag{14}$$

where $\Delta x_{PW} = x_W - x_P$, ..., and

$$\begin{aligned} A &= \Delta y_{12}\,\Delta x_{Pe} + \Delta y_{23}\,\Delta x_{Pn} \\ &\quad + \Delta y_{34}\,\Delta x_{Pw} + \Delta y_{41}\,\Delta x_{Ps} \\ &= -(\Delta x_{12}\,\Delta y_{Pe} + \Delta x_{23}\,\Delta y_{Pn} \\ &\quad + \Delta x_{34}\,\Delta y_{Pw} + \Delta x_{41}\,\Delta y_{Ps}). \end{aligned}$$

Clearly, nonuniformity can introduce false fluxes which may in turn induce a problem of consistency. This result is analogous to those obtained by Turkel [18] and Pike [16] in their analyses of one-dimensional systems.

In uniform grid systems, it is well known that the first-order upwind scheme of the convective term introduces large artificial viscosity which is represented by second-order derivatives. In nonuniform grid systems, this artificial viscosity is also contributed to by grid nonuniformity and errors due to the Newton–Cotes integration. These errors are noted by "..." in coefficients of second-order derivatives, enclosed by [ ] of Eq. (14).

By extending Turkel's [18] one-dimensional concept of consistency to the model equation, the criteria for the classicial first-order upwind scheme are

$$\begin{aligned} \Delta x_{PW}\,\Delta y_{34} + \Delta x_{PS}\,\Delta y_{41} - A &\sim O(A^{1.5}) \\ \Delta y_{PW}\,\Delta y_{34} + \Delta y_{PS}\,\Delta y_{41} &\sim O(A^{1.5}) \\ \Delta x_{PW}\,\Delta x_{34} + \Delta x_{PS}\,\Delta x_{41} &\sim O(A^{1.5}) \\ \Delta y_{PW}\,\Delta x_{34} + \Delta y_{PS}\,\Delta x_{41} + A &\sim O(A^{1.5}), \end{aligned} \tag{15}$$

where $A \leqslant A_{\max}$, and $A_{\max}$ is normalized so that the area of the whole domain is $O(1)$. As in Eq. (3), these criteria are also the reciprocal criteria of the classical first-order upwind scheme.

Turkel [17] defines the quasi-uniformity conditions of mesh systems to be

$$\begin{aligned} (\Delta x)_i/(\Delta x)_{i+1} &= 1 + O(\sqrt{A}) \\ (\Delta y)_i/(\Delta y)_{i+1} &= 1 + O(\sqrt{A}), \end{aligned} \tag{16}$$

where $(\Delta x)_i$, $(\Delta x)_{i+1}$ can be: (1) two successive grid intervals, (2) two opposite grid sides, (3) volumes of two adjacent cells, or (4) angles of two adjacent cells. By properly interpreting these conditions, it can be shown that the quasi-uniformity conditions of Eq. (16) satisfy the criteria of Eq. (15).

Next, we consider the classical second-order upwind scheme, $\overline{(\phi u)}_e = \frac{1}{2}[3(\phi u)_P - (\phi u)_W]$, ..., which is defined on the computational domain. This approximation is generally of first-order accuracy except on uniform and quasi-uniform grid systems [16, 17]. After obtaining the Taylor series expansion of the second-order upwind scheme, the coefficients α_i, β_i and the error in the convective terms can be determined. The consistency problem will again be trivial if the following criteria are satisfied:

$$\begin{aligned} &\tfrac{1}{2}[-\Delta x_{PW}\,\Delta y_{12} - \Delta x_{PS}\,\Delta y_{23} \\ &\qquad + (3\,\Delta x_{PW} - \Delta x_{P-WW})\,\Delta y_{34} \\ &\qquad + (3\,\Delta x_{PS} - \Delta x_{P-SS})\,\Delta y_{41} - 2A] \sim O(A^{1.5}) \\ &\tfrac{1}{2}[-\Delta y_{PW}\,\Delta y_{12} - \Delta y_{PS}\,\Delta y_{23} \\ &\qquad + (3\,\Delta y_{PW} - \Delta y_{P-WW})\,\Delta y_{34} \\ &\qquad + (3\,\Delta y_{PS} - \Delta y_{P-SS})\,\Delta y_{41}] \sim O(A^{1.5}) \\ &\tfrac{1}{2}[-\Delta x_{PW}\,\Delta x_{12} - \Delta x_{PS}\,\Delta x_{23} \\ &\qquad + (3\,\Delta x_{PW} - \Delta x_{P-WW})\,\Delta x_{34} \\ &\qquad + (3\,\Delta x_{PS} - \Delta x_{P-SS})\,\Delta x_{41}] \sim O(A^{1.5}) \\ &\tfrac{1}{2}[-\Delta y_{PW}\,\Delta x_{12} - \Delta y_{PS}\,\Delta x_{23} \\ &\qquad + (3\,\Delta y_{PW} - \Delta y_{P-WW})\,\Delta x_{34} \\ &\qquad + (3\,\Delta y_{PS} - \Delta y_{P-SS})\,\Delta x_{41} + 2A] \sim O(A^{1.5}). \end{aligned} \tag{17}$$

In addition to these conditions, for the scheme to be second-order accurate, the coefficients of the second-order derivatives $(u_{xx})_P$, ... must be of $O(A^2)$. Note that Turkel's quasi-uniformity conditions of Eq. (16) also fulfill Eq. (17).

Although Turkel's quasi-uniformity conditions can be easily applied, they cannot provide enough information for comparison between the first- and second-order upwind schemes. In order to understand their difference, assuming that the grid is smooth enough, the Taylor series expansions for Eq. (15) and Eq. (17) must be performed on the computational domain. According to Fig. 1b, the direction of **32**, **41** and **12**, **43** are defined by ξ and η, respectively. By taking $\Delta\xi = \Delta\eta = 1$, it follows that Eq. (15) simplifies to

$$d(\Delta x)/d\xi,\ d(\Delta x)/d\eta,\ \ldots \sim O(\sqrt{A}) \tag{18}$$

while Eq. (17) becomes

$$\begin{aligned} &d^2(\Delta x)/d\xi^2,\ d^2(\Delta x)/d\eta^2,\ d^2(\Delta x)/(d\xi\,d\eta),\ \ldots \\ &\qquad \sim O(\sqrt{A}). \end{aligned} \tag{19}$$

After comparing Eq. (18) with Eq. (19), it is evident that the error of the second-order upwind scheme will become smaller than that of the first-order upwind scheme, provided that the grid distribution is smooth enough.

In order to determine if the second-order upwind scheme still takes precedence over the first, imagine a worst case

scenario in which the grid system is stretched in the x-direction and is uniform in the y-direction, so that Δx_{PS}, $\Delta x_{P-SS}=0$ and $\Delta y_{12}=-\Delta y_{34}$. The first equation in Eq. (15) then simplifies to

$$|\Delta x_{WP}-\Delta x_{32}| \sim O([\Delta x_{23}]^2). \tag{20}$$

In a similar manner the first equation of Eq. (17) becomes

$$|-2\,\Delta x_{WP}-0.5\,\Delta x_{WW-P}-\Delta x_{32}| \sim O([\Delta x_{23}]^2). \tag{21}$$

Through application of the Taylor series expansion, it is relatively easy to obtain expressions similar to Eqs. (18) and (19). If the grid system deteriorates, the possibility of violating Eq. (21) is obviously larger than that of violating Eq. (20). In other words, the potential exists for the classical second-order scheme to introduce more false fluxes than the classical first-order upwind scheme, whenever the grid system is poor.

From the above two examples, it is intuitive that higher order approximations to u_e, v_e, ... should be considered on

error on each side of the Newton–Cotes open-end integration formulation is of second order as shown in Eq. (8a). Therefore, a second-order upwind approximation to u_e, v_e, ... seems more appropriate. For the case with positive contravariant velocity at boundary $\overline{12}$, a strictly second-order approximation for u_e would be

$$\overline{u_e}=(1-b-c)\,u_P+bu_5+cu_6, \tag{22}$$

where points 5 and 6 are centers of line segments $\overline{W-NW}$ and $\overline{W-SW}$, respectively, as shown in Fig. 1b, and

$$b=[-\Delta x_{eP}\,\Delta y_{P6}+\Delta y_{eP}\,\Delta x_{P6}]/J$$
$$c=[\Delta x_{eP}\,\Delta y_{P5}-\Delta y_{eP}\,\Delta x_{P5}]/J$$
$$J=\Delta x_{P5}\,\Delta y_{P6}-\Delta y_{P5}\,\Delta x_{P6}.$$

Similar expressions for v_e, u_n, ... can easily be derived.

According to the authors' numerical experiments and local linearized spectral approximation, the stability behavior of Eq. (22) is slightly better than the classical second-order upwind scheme. After applying the fundamental lemma, the leading error terms are composed of u_{xx}, u_{xy}, ... Thus the scheme is at least first-order accurate, avoiding the consistency problem. For the scheme to be second-order accurate, either the coefficients of all the second-order derivatives must be of $O(A^2)$ or the grid distribution must satisfy either Eq. (16) or Eq. (18). Since the grid size is finite, artificial viscosity is still present. To eliminate dissipation due to grid nonuniformity, strictly third-order approximations for u_e, ... (which results in a strictly second-order approximation for the convective term) are necessary as indicated in Pike's one-dimensional finite difference study [16].

2.5. Error Analysis of the Diffusive Term of the Model Equation

So far, the expression of the diffusive term (the Laplace operator) for the finite volume method has not been clearly studied elsewhere. In this section, a systematic approach will be demonstrated to explain the geometrical interpretation of the metric coefficients. Note that the vector $\mathbf{V}$ in Eq. (5) is replaced by $\nabla\phi$, and the lemma is applied accordingly.

For convenience, consider the discretized form of the boundary $\overline{12}$ (Fig. 1b) or S_e below,

$$\int_{S_e}\nabla\phi\cdot d\mathbf{S}=\left(\frac{\partial\phi}{\partial x}\right)_e\Delta y_{12}-\left(\frac{\partial\phi}{\partial y}\right)_e\Delta x_{12}$$

where the $\mathbf{r}_{12}$ term is a vector measured from point "1" to point "2", and $|\mathbf{r}_{12}|=\sqrt{\Delta x_{12}^2+\Delta y_{12}^2}$. Again, the error of the approximation of the line integral includes: (1) the omitted term $O(|\mathbf{r}_{12}|^3)$ and (2) the error of evaluating $[\phi_x]_e$, $[\phi_y]_e$. The following subsections will demonstrate how to interpret the latter error.

2.5.1. *The Case with Known ϕ's at Points 1, 2, P, E, ...*

Consider the cell center formulation in which the variable ϕ's at the four points 1, 2, P, E are known. The Taylor series expansions of points 1, 2, P, E are rewritten to be equations of $(\phi_2-\phi_1)$ and $(\phi_E-\phi_P)$ so that unique solutions of $[\phi_x]_e$ and $[\phi_y]_e$ can be obtained. Consequently, Eq. (23) becomes

$$\int_{S_e}\nabla\phi\cdot d\mathbf{S}=(\phi_E-\phi_P)[\Delta y_{12}\,\Delta y_{12}+\Delta x_{12}\,\Delta x_{12}]/J_0$$
$$+(\phi_2-\phi_1)[-\Delta x_{PE}\,\Delta x_{12}$$
$$-\Delta y_{PE}\,\Delta y_{12}]/J_0+\mathrm{TE1}, \tag{24a}$$

where J_0 corresponds to the Jacobian of the finite difference method. Geometrically, J_0 is equal to the area of a parallelogram with each side passing through points 1, 2, P, E and parallel to line $\overline{12}$ or $\overline{PE}$. This formula shows that the Jacobian of a finite volume method is not just an interpolation from J_E and J_P but rather a quantity defined at the surface. TE1 of Eq. (24a) denotes the error of approximation, which is

$$\mathrm{TE1} = \frac{(\phi_{xx})_e}{2}\Omega_e + (\phi_{xy})_e \Lambda_e + \frac{(\phi_{yy})_e}{2}\Theta_e + O(|\mathbf{r}_{12}|^3)$$

$$\begin{aligned}
\Omega_e &= (\Delta x_{eE}^2 - \Delta x_{eP}^2)(-\Delta y_{12}\Delta y_{12} - \Delta x_{12}\Delta x_{12})]/J_0 \\
\Lambda_e &= (\Delta x_{eE}\Delta y_{eE} - \Delta x_{eP}\Delta y_{eP}) \\
&\quad \times (-\Delta y_{12}\Delta y_{12} - \Delta x_{12}\Delta x_{12})]/J_0 \\
\Theta_e &= (\Delta y_{eE}^2 - \Delta y_{eP}^2) \\
&\quad \times (-\Delta y_{12}\Delta y_{12} - \Delta x_{12}\Delta x_{12})]/J_0.
\end{aligned} \tag{24b}$$

Equation (24a) can be interpreted by geometrical relations as

$$\int_{Se} \nabla\phi \cdot d\mathbf{S} = |\mathbf{r}_{12}| \left[(\phi_E - \phi_P) \frac{|\mathbf{r}_{12}|}{\mathbf{r}_{PE} \times \mathbf{r}_{12} \cdot \mathbf{k}} + (\phi_2 - \phi_1) \frac{-|\mathbf{r}_{PE}| \cos\theta}{\mathbf{r}_{PE} \times \mathbf{r}_{12} \cdot \mathbf{k}} \right] + \mathrm{TE1}. \tag{25}$$

The corresponding nodal locations and the angle definitions are shown in Fig. 2. The $|\mathbf{r}_{12}|$ term outside the bracket [ ] of the RHS denotes the magnitude of the control surface, while those $|\mathbf{r}_{12}|$ terms within the bracket [ ] are due to the interpolation. The first term within the bracket [ ] can be interpreted as the property variation across the cell surface while the second term is the result from the non-orthogonality of the grid system. From Fig. 2, it can be calculated that Ω, Λ, Θ take smaller values in orthogonal grid systems ($\theta = 90°$), leading to a smaller truncation error whenever the grid is smooth enough.

After writing the integrations over line segments $\overline{23}$, $\overline{34}$, and $\overline{41}$ and employing the fundamental lemma, errors of the approximation to the RHS of Eq. (13) can be determined. These errors will induce a consistent problem, except when a two-dimensional grid system has the character

$$\begin{aligned}
[\Omega_e + \Omega_n + \Omega_w + \Omega_s] &\sim O(A^{1.5}) \\
[\Lambda_e + \Lambda_n + \Lambda_w + \Lambda_s] &\sim O(A^{1.5}) \\
[\Theta_e + \Theta_n + \Theta_w + \Theta_s] &\sim O(A^{1.5}),
\end{aligned} \tag{26}$$

where Ω_n, Ω_w, Ω_s, Λ_n, Λ_w, Λ_s, Θ_n, Θ_w, and Θ_s are defined on surfaces S_n, S_w, and S_s, respectively, their forms being similar to Ω_e, Λ_e, and Θ_e in Eq. (24b).

If Turkel's quasi-uniformity conditions (Eq. (16)) are employed, it is easy to show that the criteria of Eq. (26) are fulfilled. On the other hand, analysis on the computational domain for Eq. (26) shows that this equation is equivalent to Eq. (19). For this scheme to be second-order accurate, the term, $O(A^{1.5})$, in Eq. (26) should be changed to $O(A^2)$. This property is consistent with one-dimensional analyses [8, 11, 13, 16, 17]. Moreover, additional constraints require either that the coefficients of all the third-order derivatives $(\phi_{xxx})_P \cdots$ are of $O(A^2)$ or that Eq. (16) is satisfied.

Whether or not Eq. (26) is satisfied, these terms will play a certain role in creating additional artificial viscosity whenever the grid size is finite. In other words, this dissipation cannot be avoided if one employs the finite volume method on a general grid system.

2.5.2. *The Case with Interpolation Errors at Points* 1, 2, 3, 4

In the previous subsection it was assumed that the expressions ϕ_1 and ϕ_2 were known. For a cell center formulation, however, we only know variables at the nodal points P, E, N, and NE. Interpolation of ϕ of nodal points 1, 2 from the neighbouring nodes should account for the interpolation error. First, consider the convenient approximations [1],

$$\begin{aligned}
\overline{\phi_2} &= (\phi_{NE} + \phi_N + \phi_P + \phi_E)/4 \\
\overline{\phi_1} &= (\phi_{SE} + \phi_S + \phi_P + \phi_E)/4,
\end{aligned} \tag{27}$$

where $\overline{\phi_2}$ and $\overline{\phi_1}$ are approximate values for ϕ_2 and ϕ_1. Using the Taylor expansion around the nodes 2, 1 respectively for ϕ_2, ϕ_1, ϕ_N, and so on, we obtain

$$\overline{\phi_2} - \overline{\phi_1} = \phi_2 - \phi_1 + \delta x_2 \cdot (\phi_x)_2 - \delta x_1 \cdot (\phi_x)_1 + \delta y_2 \cdot (\phi_y)_2 - \delta y_1 \cdot (\phi_y)_1 + \cdots, \tag{28}$$

where $\delta x_1 = (x_{SE} + x_S + x_P + x_E)/4 - x_1$, $\delta y_1 = (y_{SE} + y_S + y_P + y_E)/4 - y_1$, etc.

By substituting Eq. (28) into Eq. (24) and employing the fundamental lemma, it follows that

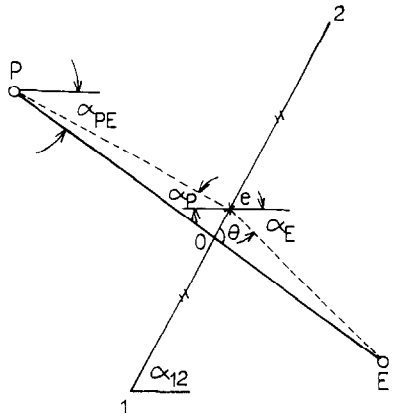

FIG. 2. The node locations and the angle definitions.

$$\text{Discrete}\left[\oint_S \nabla\phi \cdot d\mathbf{S}\right]$$
$$= \int_A \nabla^2\phi \, dA$$
$$+ (\phi_x)_P [(-\Delta x_{PE}\Delta x_{12} - \Delta y_{PE}\Delta y_{12})$$
$$\times (\delta x_2 - \delta x_1)/J_0 + \cdots]$$
$$+ (\phi_y)_P [(-\Delta x_{PE}\Delta x_{12} - \Delta y_{PE}\Delta y_{12})$$
$$\times (\delta y_2 - \delta y_1)/J_0 + \cdots]$$
$$+ (\text{terms involving } \Omega_e, \ldots) + \cdots \quad (29)$$

Consequently, the classical arithmetic average scheme of Eq. (27) will introduce significantly large false fluxes, unless the following criteria are satisfied:

$$(-\Delta x_{PE}\Delta x_{12} - \Delta y_{PE}\Delta y_{12})(\delta x_2 - \delta x_1)/J_0, \ldots \sim O(A^{1.5})$$
$$(-\Delta x_{PE}\Delta x_{12} - \Delta y_{PE}\Delta y_{12})(\delta y_2 - \delta y_1)/J_0, \ldots \sim O(A^{1.5}). \quad (30)$$

Other consistency conditions are represented by Eq. (26). Recall that the term $(-\Delta x_{PE}\Delta x_{12} - \Delta y_{PE}\Delta y_{12})$ reflects the orthogonality. For an orthogonal grid system, the deficiencies of false fluxes are trivial, but the additional numerical diffusion still depends on $\delta x_2 - \delta x_1, \ldots$. In Section 3, two test problems on a generalized grid system will show that these false fluxes reduce the accuracy of Laplace's equation solutions.

Although the terms $\overline{\phi_1}$, $\overline{\phi_2}$ (Eq. (27)), are relatively simple, they introduce an additional error. Fortunately, proper interpolations can avoid the constraints of Eq. (30). One such choice involves interpolating point "1" from points *P*, *E*, *S*, *SE*, etc. This leads to many possible froms of interpolation with second-order accuracy. After applying the fundamental lemma, the expressions of the final error form of these interpolation schemes can easily be determined. Surprisingly enough, their consistency conditions are comparable to those found in Eq. (26), Eq. (16), and Eq. (19), although artificial viscosity still plays an important role in error determination. In addition to interpolation schemes, the next section also introduces a non-interpolating method.

2.5.3. *A Proposed Finite Volume Formulation for the Diffusive Term*

In order to avoid the interpolation method for finding ϕ_1, ϕ_2, points *A*, *B* are used instead of points 1, 2. As shown in Fig. 3, points *A* and *B* are located at the arithmetic centers of four adjacent nodes *N*, *NE*, *P*, *E* and *S*, *SE*, *P*, *E*, respectively. The first-order derivatives $(\phi_x)_e$ and $(\phi_y)_e$ are now

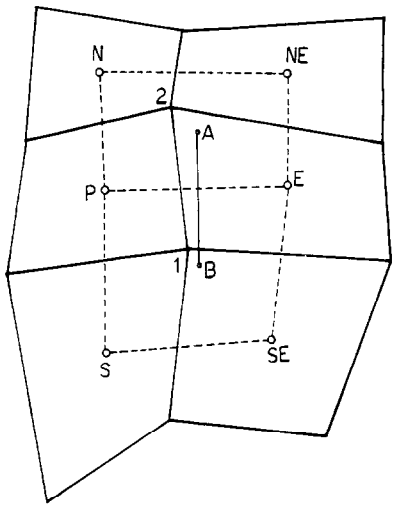

FIG. 3. The locations of A and B on the physical domain.

approximated from nodes *P*, *E*, *A*, and *B*. By applying the Taylor series expansion, their expressions become

$$\phi_A = (\phi_{NE} + \phi_N + \phi_P + \phi_E)/4 + \text{second-order error}$$
$$\phi_B = (\phi_{SE} + \phi_S + \phi_P + \phi_E)/4 + \text{second-order error} \quad (31)$$

and δx and δy of Eq. (28) will be zero. The discretized diffusive term becomes

$$\int_{Se} \nabla\phi \cdot d\mathbf{S} = (\phi_E - \phi_P)[\Delta y_{AB}\Delta y_{21} + \Delta x_{AB}\Delta x_{21}]/J_1$$
$$+ (\phi_A - \phi_B)[-\Delta x_{EP}\Delta x_{21}$$
$$- \Delta y_{EP}\Delta y_{21}]/J_1 + \text{TE2}$$
$$J_1 = \Delta y_{AB}\Delta x_{EP} - \Delta y_{EP}\Delta x_{AB} \quad (32)$$

and the problem of false fluxes disappears. The Jacobian J_1 is interpreted as the area of the parallelogram with each side passing through points *P*, *E*, *A*, *B* and parallel to line $\overline{AB}$ or $\overline{PE}$. Although this type of finite volume method slightly deviates from the finite difference method, the deviation becomes trivial whenever the grid system is uniform. The minor extra computing time for Eq. (32) is due to the determination of coordinates at four average points x_A, y_A, etc.

The form of TE2 is similar to that of TE1. If Turkel's quasi-uniformity condition is substituted, the consistency problem can be avoided. However, should the analysis on the computational domain be performed for TE2, the consistency criteria is now represented by Eq. (18) rather than by Eq. (19).

If a cell vertex formulation is employed, the problem of interpolating point values at 1, 2, 3, 4 turns out to be just the interpolation of point values at centroids *P*, *E*, ... Its accuracy is comparable to the present scheme but is better

under nonuniform grid conditions than the classical cell center scheme which makes use of Eq. (27) in its derivation. If, however, the grid system remains close to uniformity, it can be shown [23] that the difference between the cell vertex formulation and the classical cell center formulation is not significant.

Unfortunately, both the cell vertex and cell center formulation methods present specific problems in their use and it is difficult to determine which is more suited to solving the diffusive term. For instance, in order to cancel the error associated in unsteady computation of the cell vertex formulation, some additional computations must be made [20]. And in the case of the cell center formulation, either A, B must be determined or the interpolation of 1, 2, 3, 4 undertaken.

If one wants to eliminate the consistency problem completely, it is obvious that higher order approximations for $(\phi_x)_e$ and $(\phi_y)_e$ are necessary [36, 37]. For example, to obtain second-order accurate approximations for ϕ_x and ϕ_y, six independent equations formed by neighbouring nodal points are needed to evaluate $(\phi)_e$ and the five different derivatives at point "e". In other words, one must invert a 6×6 matrix. For a nonoverlapping quadrilateral grid system, the coefficient matrix is non-singular [37] and the derivatives can be solved by techniques of matrix inversion such as Gaussian elimination, etc. Unfortunately, the matrix inversion will significantly increase the required computer resource, which destroys the fast and simple nature of finite volume methods. Moreover, when we consider the error sources of discretization for the convective term and the interpolations for nodes ϕ_e, ϕ_n, ϕ_w, and ϕ_s, we should also take into consideration the overall order of accuracy. Therefore, in order to avoid consistency problems, one has to simultaneously employ a high order interpolation formula and a high order integration formula for both the convective and the diffusive terms.

3. APPLICATION TO THE LAPLACE EQUATION

The Laplace equation with Dirichlet boundary on the unit square and the unit circle, as shown in Figs. 4 and 5, respectively, is studied. The boundary conditions are chosen so that exact solutions exist. The test problem for convective and diffusive terms will be demonstrated in a forthcoming manuscript concerning the SIMPLER type algorithm on a staggered grid system [35]. A proposed scheme for diffusive terms as well as four additional schemes are:

(1) the classical finite difference method by coordinate transformation [38].

(2) the classical finite volume method [1, 39] of Eq. (24a) with the interpolation of Eq. (27).

(3) a modification of scheme (2). The metric coefficients are first evaluated by central differencing at grid nodes P, E, W, N, S, ... and then interpolated to give the desired metric coefficients at points corresponding to e, n, w, ... [40].

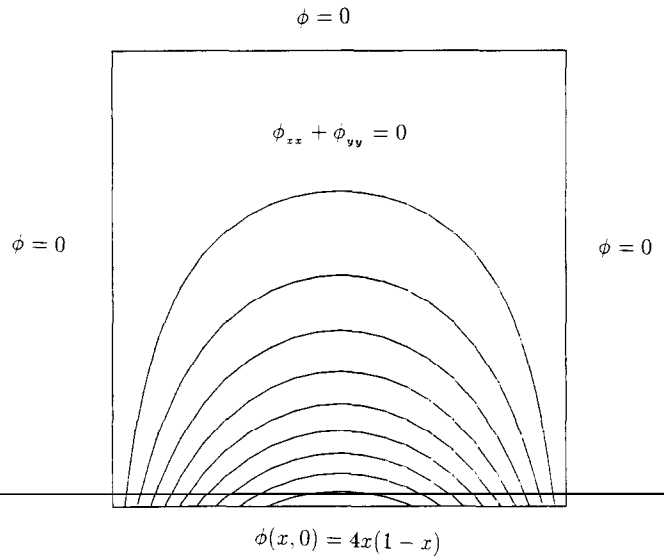

FIG. 4. The constant property contours of the unit square problem.

(4) the finite volume method of Eq. (24a) with the interpolation algorithm [41] which extends the existing methods for regular grids to grids consisting of non-equidistant convex four-point meshes.

(5) the finite volume method of Eq. (32) with the interpolation of Eq. (31). This is the proposed method.

All schemes are performed on 21×21 grid systems on the VAX-785 with double precision programming. The convergence criterion is set to be less than 1×10^{-12} in each case.

For comparison, several grid systems are employed. The

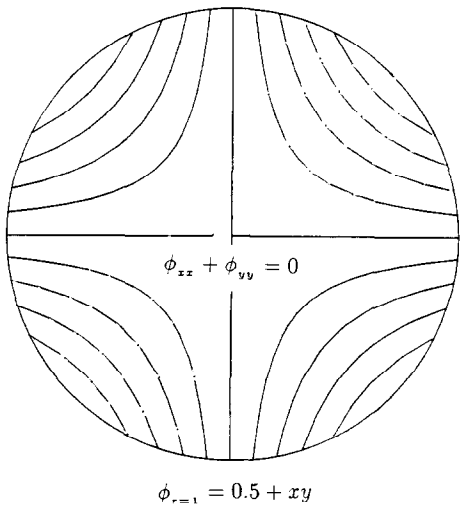

FIG. 5. The constant property contours of the unit circle problem.

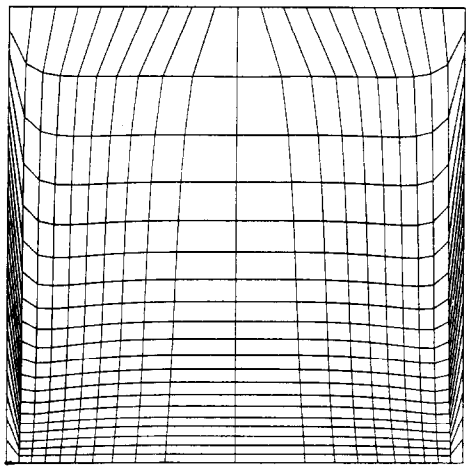

FIG. 6. Grid A generated by the multiple one-dimensional adaptive grid scheme.

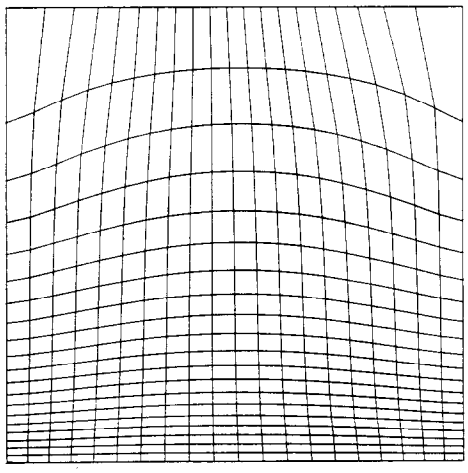

FIG. 7. Grid B generated by the modified multiple one-dimensional adaptive grid scheme.

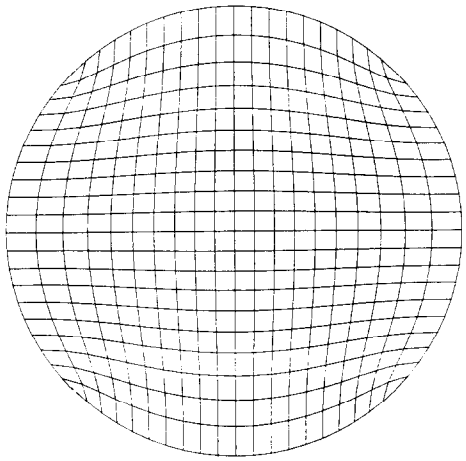

FIG. 8. Grid C generated by Thomas and Middlecoff's method.

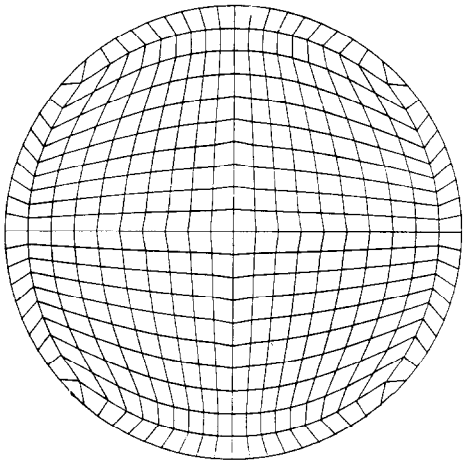

FIG. 9. Grid D generated by the multiple one-dimensional adaptive grid scheme.

result of employing the single line multiple one-dimensional adaptive grid scheme of Shyy [38, 42] along the ξ-direction first and then along the η-direction is shown in Fig. 6. The initial data for grid adaption is solved on a uniform grid system. The grid adaption along a grid line $\eta = \eta_j$ uses the identity

$$\xi_{i,j} = \frac{\sum_{i=1}^{i} [1 + \lambda\, |\phi_{i,j} - \phi_{i-1,j}|/|s_{i,j} - s_{i-1,j}|][s_{i,j} - s_{i-1,j}]}{\sum_{i=1}^{i_{\max}} [1 + \lambda\, |\phi_{i,j} - \phi_{i-1,j}|/|s_{i,j} - s_{i-1,j}|][s_{i,j} - s_{i-1,j}]}, \tag{33}$$

where "s" is the arc length along a known grid line, and the parameter "λ" is taken to be "20." The grid distortion is more serious near the left and right boundaries. The adaptive grid technique [38] is employed to smooth out the grid distortion (see Fig. 7). It makes use of $\nabla\phi$ to replace $\Delta\phi/\Delta s$ and averages over three grid lines by Simpson's rule,

$$\begin{aligned} \xi_{i,j} &= \frac{\sum_{i=1}^{i} [1 + \lambda\, |\nabla\phi^0_{i,j}|][s_{i,j} - s_{i-1,j}]}{\sum_{i=1}^{i_{\max}} [1 + \lambda\, |\nabla\phi^0_{i,j}|][s_{i,j} - s_{i-1,j}]} \\ |\nabla\phi^0_{i,j}| &= \tfrac{1}{6}[|\nabla\phi_{i,j-1}| + 4\,|\nabla\phi_{i,j}| + |\nabla\phi_{i,j+1}|], \end{aligned} \tag{34}$$

TABLE I

Comparison of Numerical Errors on Grid A for a Unit Square

Scheme	$\phi_{\max}$	$\tilde{\phi}_{\max}$	$E_{\max}$	E_{rms}
1	0.94140174	0.94822249	1.98925569E-2	1.08832162E-2
2	0.94729400	0.95053805	7.65071752E-3	3.29574456E-3
3	0.94729400	0.94966534	2.01228672E-2	4.57252834E-3
4	0.94729400	No solution	No solution	No solution
5	0.94729400	0.95041010	7.02103965E-3	2.60045986E-3

Note. $\tilde{\phi}$ is the numerical approximation; ϕ is the exact solution; $E_{\max} = \max\, |\tilde{\phi} - \phi|/\phi_{\max}$; $E_{\text{rms}} = [1/(I \times J) \sum_I \sum_J (\tilde{\phi} - \phi)^2]^{1/2}/\phi_{\max}$.

TABLE II

Comparison of Numerical Errors on Grid B for a Unit Square

Scheme	$\phi_{\max}$	$\tilde{\phi}_{\max}$	$E_{\max}$	E_{rms}
1	0.85070941	0.85374261	1.301988073E-2	9.58781016E-4
2	0.92094750	0.92267935	1.01903404E-2	1.98882378E-3
3	0.92094750	0.92194976	1.58647704E-2	2.87263707E-3
4	0.92094750	0.92242128	4.38156269E-3	1.21964658E-3
5	0.92094750	0.92243125	6.41224183E-3	1.52879073E-3

TABLE IV

Comparison of Numerical Errors on Grid D for a Unit Circle

Scheme	$\phi_{\max}$	$\tilde{\phi}_{\max}$	$E_{\max}$	E_{rms}
1	0.94141127	0.93130423	2.10540432E-2	6.87198556E-3
2	0.98350507	0.98468635	6.61281701E-3	1.76685491E-3
3	0.98350507	0.98502009	1.10147813E-2	2.68308239E-3
4	0.98350507	0.98458861	2.71664869E-3	8.46870876E-4
5	0.98350507	0.98428891	2.17046141E-3	6.64613902E-4

where the $\nabla\phi_{i,j}$ terms are evaluated by a central difference scheme on the computational domain, and $\lambda = 20$. The grid distribution of a unit circle generated by Thomas and Middlecoff's scheme [43] is shown in Fig. 8. The resultant solution was used to generate the relatively poorer adaptive grid system of Fig. 9 with respect to that of Fig. 8.

The resultant solution errors of the grid system of Fig. 6 are shown in Table I. In scheme 4, the results of "no solution" can be explained due to the fact that grid distortion has shifted the average position of point 2. Point 2 of Fig. 1b is now located outside the quadrilateral region with vertices *P*, *E*, *NE*, and *N*. In the case of the proposed model (scheme 5), minimum error is achieved while that of the classical model (scheme 1) exhibits maximum error.

The resultant solution errors of the smooth grid system of Fig. 7 are shown in Table II. In comparison to Table I, the errors of all the schemes are reduced. Furthermore, it is interesting to note that while the accuracy of schemes 1–4 are relatively sensitive to grid distortion, the proposed model (scheme 5) is not.

The resultant solution errors of the smooth grid system of Fig. 8 are shown in Table III, while Table IV lists those calculations obtained from the slightly skewed grid of Fig. 9. In this particular case, the accuracy of schemes 1–3 are relatively sensitive to grid distortion, whereas the fourth and fifth schemes are not.

In summary, it was shown that all the schemes outlined can produce good results, but only if those conditions that generate smooth grid systems are met. However, when the grids become distorted, the classical finite difference model (scheme 1) deteriorates in terms of accuracy and becomes the worst one of the series. Under these distorted grid conditions, the direct average model (scheme 2) and the modified finite volume model (scheme 3) fair a little better in comparison to scheme 1, but by far the two best schemes are the interpolation model (scheme 4) and the proposed model (scheme 5). Unfortunately, the interpolation model sometimes has "no solution" as in the case in Table I.

TABLE III

Comparison of Numerical Errors on Grid C for a Unit Circle

Scheme	$\phi_{\max}$	$\tilde{\phi}_{\max}$	$E_{\max}$	E_{rms}
1	0.95453782	0.95605050	1.64873710E-3	6.33302504E-4
2	0.98690919	0.98900893	2.09994450E-3	6.08649825E-4
3	0.98690919	0.98804812	2.75684992E-3	1.19452859E-3
4	0.98690919	0.98832047	1.41142622E-3	5.20898807E-4
5	[illegible]	[illegible]	[illegible]	[illegible]

4. CONCLUSIONS

A fundamental error relation of discretizing the line integral part of the Gauss divergence theorem is summarized into a lemma. Based on this lemma and on a generalized grid system, the classical first- and second-order upwind schemes of the finite volume method for convective terms are proved to be at most first order on the physical domain, provided that the grid distribution is subject to certain constraints. A proposed scheme is found to be of first-order accuracy.

The finite volume method for the diffusive term is systematically studied. It is found that the interpolation concept plays a key role and that the order of accuracy depends on the interpolation process. The classical averaging method for diffusive terms introduces false fluxes and can be adjusted either by proper interpolations or by a proposed modification. All the discussed schemes are consistent with the Laplace operator provided the grid distribution is subject to certain constraints. Five schemes, including the proposed scheme for the diffusive term, are examined for two test cases of the Laplace equation. Among the studied schemes, the proposed scheme for the diffusive term achieves the highest accuracy as well as being less sensitive to moderate grid distortion.

REFERENCES

1. M. Vinokur, *J. Comput. Phys.* **81**, 1 (1989).
2. R. D. Richtmyer and K. W. Morton, *Difference Methods for Initial-Value Problems* (Wiley, New York, 1967), p. 45.
3. T. Cebeci and A. M. O. Smith, in *Proceedings, Computation of Turbulent Layers 1968*, AFOSR-IFP Stanford Conference [illegible]

4. S. V. Patankar and D. B. Spalding, *Int. J. Heat Mass Transfer* **10**, 1389 (1967).
5. A. Arakawa, *J. Comput. Phys.* **1**, 119 (1966).
6. E. Kalnay de Rivas, *J. Comput. Phys.* **10**, 202 (1972).
7. T. Cebeci and A. M. O. Smith, *Analysis of Turbulent Boundary Layers* (Academic Press, London, 1974), p. 330.
8. F. G. Blottner, *Comput. Methods Appl. Mech. Eng.* **4**, 179 (1974).
9. C. W. Hirt and J. D. Ramshaw, "Prospects for Numerical Simulation of Bluff-Body Aerodynamics," in *Aerodynamic Drag Mechanisms of Bluff Bodies and Road Vehicles*, edited by G. Sovran, T. Morel, and W. Mason, Jr. (Plenum, New York, 1978).
10. P. J. Roache, *Computational Fluid Dynamics* (Hermosa, Albuquerque, NM, 1976), p. 295.
11. J. D. Hoffman, *J. Comput. Phys.* **46**, 469 (1982).
12. J. F. Thompson, Z. U. A. Warsi, and C. W. Mastin, *J. Comput. Phys.* **47**, 1 (1982).
13. J. F. Thompson and C. W. Mastin, "Order of Difference Expressions in Curvilinear Coordinate Systems," in *Advances in Grid Generation*, edited by K. N. Ghia and U. Ghia (ASME, New York, 1983).
14. D. Lee and Y. M. Tsuei, *J. Comput. Phys.*, in press.
15. J. P. Veuillot and H. Viviand, AIAA Paper 78-1150, Washington, 1978 (unpublished).
16. J. Pike, *J. Comput. Phys.* **71**, 194 (1987).
17. E. Turkel, *Appl. Numer. Math.* **2**, 529 (1986).
18. E. Turkel, ICASE Report No. 85-43, Sept. 1985 (unpublished).
19. E. Turkel, S. Yaniv, and U. Landau, AIAA Paper 86-0341, Nevada, 1986 (unpublished).
20. P. L. Roe, ICASE Report No. 87-6, 1987 (unpublished).
21. M. B. Giles, in *Proceedings, 11th International Conference on Numerical Method in Fluid Dynamics, Williamsburg, Virginia, 1988*, edited by D. Dwoyer (Springer-Verlag, New York, 1989), p. 273.
22. J. C. T. Wang and G. F. Widhopf, *J. Comput. Phys.* **84**, 145 (1989).
23. R. Radespiel and R. Swanson, AIAA Paper 89-0548, 1989 (unpublished).
24. K. W. Morton and M. F. Paisley, *J. Comput. Phys.* **80**, 168 (1989).
25. J. Flores, T. L. Holst, D. Kwak, and D. M. Batiste, *AIAA J.* **22**, 1027 (1984).
26. D. R. Lindquist and M. B. Giles, in *Proceedings, 11th Internationa Conference on Numerical Method in Fluid Dynamics, Williamsburg Virginia, 1988*, edited by D. Dwoyer (Springer-Verlag, New York 1989), p. 369.
27. E. Süli, Oxford University Computing Laboratory, Technical Report No. 89-6, 1989; *Math. Comput.*, submitted.
28. E. Süli, Oxford University Computing Laboratory, Technical Report No. 90-7, 1990; *SIAM J. Numer. Anal.*, to appear.
29. E. Süli, in *The Mathematics of Finite Elements and Applications VII*, edited by J. Whiteman (Academic Press, London), to appear.
30. I. S. Sokolnikoff and R. M. Redheffer, *Mathematics of Physics and Modern Engineering* (McGraw–Hill, New York, 1966), p. 397.
31. F. B. Hildebrand, *Introduction to Numerical Analysis* (McGraw–Hill, New York, 1974), p. 91.
32. R. H. Ni, *AIAA J.* **20**, 1565 (1982).
33. A. Jameson and D. Mavriplis, AIAA Paper 85-0435, Nevada, 1985 (unpublished).
34. K. C. Reddy and J. L. Jacocks, AIAA Paper 87-1144, Hawaii, 1987 (unpublished).
35. S. V. Patankar, *Numerical Heat Transfer and Fluid Flow* (Hemisphere, Washington, DC/New York, 1980), p. 126.
36. G. Forsythe and W. Wasow, *Finite Difference Methods for Partial Differential Equations* (Wiley, New York, 1960), p. 175.
37. N. Perrone and R. Kao, *Computers & Structures* **5**, 45 (1975).
38. Y. N. Jeng and S. S. Liou, *Numer. Heat Transfer B* **15**, 241 (1989).
39. S. R. Chakravarthy, K. Y. Szema, U. C. Goldberg, and J. J. Gorski, AIAA Paper 85-0165, Nevada, 1985 (unpublished).
40. W. Shyy, S. S. Tong, and S. M. Correa, *Numer. Heat Transfer* **8**, 99 (1985).
41. S. David and W. Thomas, *J. Comput. Phys.* **79**, 1 (1988).
42. W. Shyy, *Appl. Math. Comput.* **21**, 201 (1987).
43. P. D. Thomas and J. F. Middlecoff, *AIAA J.* **18**, 652 (1980).